The same argument holds again for the broad state near 20 MeV. A definite state at 20.0±0.5 MeV in ^{5}Li was recently observed[15] as a D-wave d-^{3}He interaction with a tentative spin assignment of $\frac{3}{2}+$ or $\frac{5}{2}+$; the mirror level in ^{5}He has only tentative support.[8,16] Comparative (p,t) and $(p,^3\mathrm{He})$ data permit us to distinguish between the two possible total spin configurations for this state, ^{2}D and ^{4}D. The appearance of a state at 19.9±0.4 MeV in the ^{7}Li$(p,^3$He$)^5$He data and the absence of transitions to the presumed mirror level at 20 MeV in the ^{7}Li$(p,t)^5$Li data imply that the latter transition is S forbidden and that the state is $^4D_{3/2 \text{ or } 5/2}$.[17]

A careful search was made for the first $T=\frac{3}{2}$ state in the mass-5 system. No states other than those discussed above were observed. Since the lowest $T=\frac{3}{2}$ state would be expected to be a doublet in total spin, the (p,t) reaction could populate it and would be expected to be fairly sensitive—except for the high triton continuum background—because of the above-mentioned absence of other transitions in the region about 20 MeV of excitation. In order to permit a more sensitive search for a possible $T=\frac{3}{2}$ state, a coincidence experiment capable of observing the decay properties of levels of ^{5}He and ^{5}Li from 16.6- to 28-MeV excitation is in progress.

[15] T. A. Tombrello, A. D. Bacher, and R. J. Spiger, Bull. Am. Phys. Soc. **10**, 423 (1965).
[16] S. J. Bame and J. E. Perry, Phys. Rev. **107**, 1616 (1957).
[17] Preliminary results of a ^{7}Li$(p,t)^5$Li and ^{6}Li$(p,d)^5$Li experiment at 155 MeV appear to support these spin assignments. D. Bachelier, M. Bernas, I. Brissaud, F. Chavy, and P. Radvanyi (private communication).

PHYSICAL REVIEW VOLUME 152, NUMBER 3 16 DECEMBER 1966

Theory of Coulomb Disintegration of Complex Nuclei*

KÔSUKE NAKAMURA†
Department of Physics, University of California, San Diego, La Jolla, California
(Received 1 March 1966; revised manuscript received 8 July 1966)

A general formulation of the Coulomb disintegration of complex nuclei is presented using the semiclassical approximation. This assumes that the center of gravity of the incident nucleus moves along a Rutherford orbit in the Coulomb field of the target nucleus. The main point of the formulation is the following: The configuration space of the product nuclei is divided into the external region and the internal region. In the external region, the wave function is assumed to be an outgoing free spherical wave. This wave function is then connected continuously to the internal wave function, which we take, following the Kapur-Peierls method, to be a superposition of compound-state eigenfunctions of the incident nucleus. This method is applied to the Coulomb disintegration of ^{6}Li and compared with the results which Gluckstern and Breit have already obtained. Some discussion about higher order corrections, which modify considerably the first-order perturbation calculation in the case of ^{6}Li, and about the stripping mechanism is added.

I. INTRODUCTION

THE study of the interaction of two complex nuclei is a newly developed field of research, in which theoretical results remain very few, in contrast with the experimental results which have been accumulating very rapidly in recent years.

Theoretically, the phenomena are expected to become simplest when the distance of the closest approach of two nuclei remains larger than the sum of their radii, preventing any nuclear force from acting effectively between the incident and the target nuclei. Even in this simplest case, we can expect many interesting types of reactions because of the intense Coulomb force. For example, Coulomb excitations of the target or the incident nucleus have been studied[1] extensively, both experimentally and theoretically, and have furnished much information about the spectroscopy of the nuclei.

However, Coulomb disintegration of the nuclei, which is expected to occur with a considerable probability in collisions of complex nuclei, has not yet been studied so fully, because of some difficulties with the detection techniques. For example, when α particles are observed in some heavy-ion reactions, it is not at all simple to distinguish α particles ejected from the direct Coulomb disintegration of the incident nucleus from those provided through the evaporation of the compound nucleus, or through the stripping or knockout processes.

In this respect, theoretical investigation of the Coulomb disintegration cross section, which is relatively easy to perform compared with other, more complicated nuclear processes, might serve to eliminate Coulomb contributions and separate out purely nuclear contributions from the observed cross sections. Furthermore, as will be discussed later, we might expect rather pure Coulomb disintegration of the incident nucleus in the

* Work supported by the U. S. Atomic Energy Commission.
† On leave of absence from Tokyo University of Education, Tokyo, Japan.
[1] K. Alder, A. Bohr, T. Huus, B. Mottelson, and A. Winther, Rev. Mod. Phys. **28**, 432 (1956); K. Alder and A. Winther, Kgl. Danske Videnskab. Selskab, Mat. Fys. Medd. **32**, No. 8 (1960).

external Coulomb field of the target nucleus for lower incident energies and forward-ejection angles of the reaction products. In such situations, the angular distribution and energy distribution of the disintegration products would give information about lower unstable excited levels of the incident nucleus.

Numerous calculations have been published on the Coulomb disintegration of the deuteron[2] but we have only a few examples of calculations for complex nuclei.[3]

Recently, observations of α particles by Anderson,[4] in which a gold target was bombarded by ^{6}Li nuclei with energies from 20 to 65 MeV, were interpreted by Gluckstern and Breit[5] as a Coulomb disintegration process $^6\mathrm{Li} \rightarrow \alpha + d$. Gluckstern and Breit have assumed that, at least in the ^{6}Li case, Coulomb excitations of the lower excited levels (unstable for $^6\mathrm{Li} \rightarrow \alpha + d$) and subsequent decays are the main processes of the Coulomb disintegration. Concerning the higher order approximations, they have pointed out the effect of the finiteness of the lifetimes of the excited levels and the qualitative fits obtained for the energy distribution and the angular distribution seem to be convincing proof of their above mentioned assumptions, though some details of the anisotropy of the directional distribution of the ejected α particles are omitted in their paper.

Bearing this situation in mind, we shall give in the present paper a more general formulation of the Coulomb disintegration cross section of complex nuclei.

The center of mass of the incident nucleus is assumed to move along a Rutherford orbit in the Coulomb field of the target nucleus. This approximation is justified under the following two conditions: First, $ZZ'e^2/\hbar v_0 \gg 1$, where Z, Z' are the atomic numbers of the target and the incident nuclei, respectively, and v_0 is the incident velocity; second, the energy loss by the Coulomb excitation is very small compared with the kinetic energy of the incident nucleus. These conditions are generally satisfied in the Coulomb disintegration under consideration.

Now, the protons in the incident nucleus feel the time-dependent Coulomb forces from the target nucleus, and these perturbations may induce the splitting of the incident nucleus into two parts. The use of a plane wave for the description of the relative motion of these disintegration products is by no means adequate, because the kinetic energy of the relative motion is generally small (less than several MeV) and further, the contribution to the integral in the matrix elements of the perturbation comes mainly from the part of configuration space where the internal wave functions of the product nuclei overlap considerably.

The main point of our formulation is the following: The configuration space of the product nuclei is divided into the external region, where the relative distance of the two product nuclei is larger than a certain channel radius a_s, and the internal region, where the relative distance is smaller than a_s. In the external region, the wave function is assumed to be an outgoing spherical wave of free motion. This wave function is then connected continuously to the internal wave function, which we take, following the Kapur-Peierls method,[6] to be a superposition of the compound-state eigenfunctions of the incident nucleus.

This method very naturally leads to a generalization of the Gluckstern-Breit treatment, in the sense that the finite life times of the compound states can be fully taken into account. This point may be of greater importance when the excited states leading to the final disintegration have larger widths.

However, since the experimental data are still very scarce, we apply our differential cross sections to the $^6\mathrm{Li} \rightarrow \alpha + d$ case, already investigated by the above authors, and compare our results with theirs.

We also mention that, in some cases, first-order perturbation theory is insufficient and higher order corrections are important. Indeed, when the disintegration width of an excited level is very small, we must take account of the possibility that the incident nucleus, once excited in the Coulomb field, might be de-excited again before it has enough time to go into the final disintegrated states. Breit and Gluckstern have given an exact detailed treatment of the process.[7] We present here an alternative treatment which, though not exact, yields with very little effort corrections which modify the first-order results.

Finally, some discussion of the nuclear effect is added.

II. METHOD OF CALCULATION

As mentioned in Sec. I, the center of mass of the incident nucleus is assumed to move, even after the disintegration, in a classical orbit in the Coulomb field of the target nucleus.

For $t \rightarrow -\infty$, the incident nucleus is in its ground state J_0, M_0, described by the eigenfunction $\Psi_{J_0 M_0}$. The perturbing Coulomb potential of the target nucleus (atomic number Z) on the incident nucleus (atomic number Z')

[2] J. R. Oppenheimer, Phys. Rev. **47**, 845 (1945); S. M. Dancoff, *ibid.* **72**, 1017 (1947); L. D. Landau and E. M. Lifshitz, Zh. Eksperim. i Teor. Fiz. **18**, 750 (1948); C. J. Mullin and E. Guth, Phys. Rev. **82**, 141 (1951); Y. Nishida, Progr. Theoret. Phys. (Kyoto) **19**, 389 (1958); R. Gold and C. Wong, Phys. Rev. **132**, 2586 (1963).

[3] V. I. Mamasakhilsov and G. A. Chilashvili, Zh. Eksperim. i Teor. Fiz. **32**, 806 (1956) [English transl.: Soviet Phys.—JETP **5**, 661 (1957)]; J. M. Hansteen, Nucl. Phys. **19**, 309 (1960); J. M. Hansteen and I. Kanestrom, *ibid.* **46**, 303 (1963); J. M. Hansteen and H. W. Wittern, Phys. Rev. **137**, B524 (1965).

[4] C. E. Anderson, in *Proceedings of the Second Conference on Reactions between Complex Nuclei, 1960*, edited by A. Zucker, E. C. Halbert, and F. T. Howard (John Wiley & Sons, Inc., New York, 1960), p. 67.

[5] R. L. Gluckstern and G. Breit, in *Proceedings of the Second Conference on Reactions between Complex Nuclei, 1960*, edited by A. Zucker, E. C. Halbert, and F. T. Howard (John Wiley & Sons, Inc., New York, 1960), p. 77.

[6] P. L. Kapur and R. Peierls, Proc. Roy. Soc. (London) **A166**, 277 (1938); G. E. Brown, Rev. Mod. Phys. **31**, 893 (1959).

[7] G. Breit and R. L. Gluckstern, Nucl. Phys. **20**, 188 (1950).

is given by

$$H'=\sum_{i=1}^{Z'}\frac{Ze^2}{|\mathbf{R}-\mathbf{r}_i|}-\frac{ZZ'e^2}{R}, \tag{2.1}$$

where $\mathbf{R}$ is the position vector of the center of mass of the incident nucleus measured from that of the target nucleus, while $\mathbf{r}_i$ denotes the position vector of the ith proton in the target nucleus with respect to its center of mass. The variation of $R(t)$ with time is determined from the classical orbital motion of the projectile.

For $t\rightarrow+\infty$, the incident nucleus is supposed to be disintegrated by the perturbation H' into two fragments of mass M_1 and M_2. The probability amplitude of such disintegration is given in first-order perturbation theory by

$$b_{k,s,lm}(t)=\frac{1}{i\hbar}\int_{-\infty}^{\infty}\langle\Psi_{k,s,lm}|H'|\Psi_{J_0M_0}\rangle \times e^{-(i/\hbar)(W_0-E_k-W_s)t}dt, \tag{2.2}$$

where $\Psi_{k,s,lm}$ is the energy-normalized eigenfunction of the final state, in which product nuclei fly away with the relative momentum $\hbar k$, channel index s, and relative orbital angular-momentum quantum numbers l, m. Here $E_k=\hbar^2k^2/2\mu_s$ is the relative kinetic energy, $\mu_s=M_1M_2/(M_1+M_2)$ is the effective mass, W_s is the sum of the binding energies of the product nuclei, and W_0 is the binding energy of the incident nucleus in its ground state.

Expansion of H' into spherical harmonics gives

$$b_{k,s,lm}=\frac{4\pi Ze^2}{i\hbar}\sum_{\lambda=1}^{\infty}\sum_{\mu=-\lambda}^{\lambda}(2\lambda+1)^{-1} \times\langle\Psi_{k,s,lm}|\sum_i r_i^{\lambda}Y_{\lambda\mu}^*(\Omega_r)|\Psi_{J_0M_0}\rangle S_{\lambda\mu}, \tag{2.3}$$

with

$$S_{\lambda\mu}=\int_{-\infty}^{\infty}\frac{Y_{\lambda\mu}(\Omega_R(t))}{R^{\lambda+1}(t)}e^{i\omega_{ks}t}dt, \tag{2.4}$$

where $\hbar\omega_{ks}=E_k+W_s-W_0$, and $R(t)$, $\Omega_R(t)$ are the length and the directional angles of the vector $\mathbf{R}$. The integral $S_{\lambda\mu}$ is familiar in the study of Coulomb excitation and has been evaluated by Alder *et al.*[1]

The difference between the present reaction and Coulomb excitation is that $\Psi_{k,s,lm}$ is now not one of a set of discrete excited levels but a continuous level of the disintegrated product nuclei. The simplest approximation for $\Psi_{k,s,lm}$ would be a plane wave of relative motion for product nuclei multiplied by their internal-channel eigenfunctions; however, the main contributions to the matrix element in Eq. (2.3) arise from the part of configuration space for which $\Psi_{k,s,lm}$ overlaps strongly with the ground-state eigenfunction $\Psi_{J_0M_0}$. Thus the use of a plane wave hardly seems to be justified.

It becomes preferable, then, to represent $\Psi_{k,s,lm}$ in the important region of configuration space as a superposition of the compound-state eigenfunctions for the incident nucleus. This will be treated in the following section.

III. CALCULATION OF THE MATRIX ELEMENT

We now divide configuration space into two parts: the external region, where the relative distance $|\mathbf{r}|=r$ of two product nuclei is larger than a certain channel radius a_s, and the internal region, where r is smaller than a_s.

In the external region we choose $\Psi_{k,s,lm}$ to be a product of the energy-normalized wave function for relative motion,

$$\nu(k)[\varphi_l(kr)/r]Y_{lm}(\Omega_r), \tag{3.1}$$

with the normalization constant $\nu=(2\mu_sk/\pi\hbar^2)^{1/2}$, and the channel eigenfunction of internal variables ξ,

$$\Phi_s(\xi)=\sum_{m_1,m_2}(j_1m_1,j_2m_2|j_sm_s) \times\chi_{j_1m_1}^{(1)}(\xi_1)\chi_{j_2m_2}^{(2)}(\xi_2). \tag{3.2}$$

The χ's are the eigenfunctions of the two product nuclei, 1 and 2, with angular momenta j_i, m_i $(i=1, 2)$, while the Clebsch-Gordan coefficient $(j_1m_1,j_2m_2|j_sm_s)$ combines them into the channel eigenfunction with angular momentum j_sm_s.

Thus,

$$\Psi_{k,s,lm}=\nu(k)[\varphi_l(kr)/r]Y_{lm}(\Omega_r)\Phi_s, \quad r>a_s. \tag{3.3}$$

The radial wave function $\varphi_l(kr)$ can be taken as

$$\varphi_l(kr)=(1/2ik)[e^{i\delta_l}\varphi_l^{(+)}(kr)-e^{-i\delta_l}\varphi_l^{(-)}(kr)] \tag{3.4}$$

with

$$\varphi_l^{(+)}(kr)=ikrh_l^{(1)}(kr), \quad \varphi_l^{(-)}(kr)=-ikrh_l^{(2)}(kr).$$

The phase shift δ_l must be chosen so that $\varphi_l(kr)$ and $d\varphi_l(kr)/dr$ are connected continuously to the internal radial wave function at $r=a_s$.

If we define $\chi_{s,l,JM}(\xi,\Omega_r)$ as

$$\chi_{s,l,JM}=\sum_{m_s,m}(j_sm_s,lm|JM)\Phi_s(\xi)Y_{lm}(\Omega_r), \tag{3.5}$$

then we have an alternative expression for $\Psi_{k,s,lm}$ which is convenient for calculational purposes:

$$\Psi_{k,s,lm}=\nu(k)[\varphi_l(kr)/r]\sum_{J,M}(j_sm_s,lm|JM)\chi_{s,l,JM}. \tag{3.6}$$

We have chosen φ_l above to represent free motion, but in general, the relative momentum $\hbar k$ may be small and the influence of the Coulomb repulsion between the product nuclei may not be negligible. However, as will be shown later, this difficulty can be remedied by replacing this penetration factor with an experimental one.

Now, in the internal region, we expand $\Psi_{k,s,lm}$ into the compound-state eigenfunction Φ_{pJM} as given by

the Kapur-Peierls method, which satisfies

$$(H-W_{pJ})\Phi_{pJM}=0, \quad r<a_s$$
$$H=H(\xi)+T(R)+V(\xi). \tag{3.7}$$

$H(\xi)$ is the Hamiltonian of the internal nuclear particles of the projectile, $T(R)$ is the kinetic energy of the incident particle, and $V(\xi)$ is the interaction potential among the internal nuclear particles. The compound-state eigenfunction Φ_{pJM} is subject to the following boundary condition at $r=a_s$:

$$\int \chi_{s,l,JM}^* \frac{\partial \Phi_{pJM}}{\partial r} d\Omega_r d\xi = (f_{s,l}^{(+)} - a_s^{-1}) \int \chi_{s,l,JM}^* \times \Phi_{pJM} d\Omega_r d\xi, \tag{3.8}$$

with

$$f_{s,l}^{(+)} = \frac{1}{\varphi_l^{(+)}(k_s r)} \frac{d\varphi_l^{(+)}(k_s r)}{dr}, \tag{3.9}$$

where $\hbar k_s$ is the channel momentum. The wave function $\tilde{\Phi}_{pJM}$ is the complex conjugate of only the radial part of Φ_{pJM}. It is obtained in a similar way and is subject to the same boundary condition if we change $(+)$ in Eqs. (3.8) and (3.9) into $(-)$.

The orthogonality condition is

$$\int_{\text{int}} \tilde{\Phi}_{p'J'M'}^* \Phi_{pJM} d\tau = N_{pJ} \delta_{pp'} \delta_{JJ'} \delta_{MM'}, \tag{3.10}$$

where the constant N_{pJ} does not deviate appreciably from unity for sharp resonance levels.

Now, we put

$$\Psi_{k,s,lm} = \sum_{pJ,M} C_{kslm,pJM} \Phi_{pJM}, \quad r<a_s \tag{3.11}$$

and, using Green's theorem, the coefficients $C_{kslm,pJM}$ are found to be

$$C_{kslm,pJM} = -\frac{\hbar^2 a_s}{2\mu_s} \frac{\nu(k) e^{-i\delta_l}}{\varphi_l^{(+)}(k_s a_s)} (j_s m_s, lm | JM) \times \frac{\int \tilde{\Phi}_{pJM}^* \chi_{s,l,JM} d\Omega_r d\xi}{N_{pJ}(E_k + W_s - \mathcal{E}_{pJ} + \frac{1}{2} i \Gamma_{pJ})}, \tag{3.12}$$

where $\mathcal{E}_{pJ}$ and $\frac{1}{2}\Gamma_{pJ}$ are the real and the imaginary part of the complex eigenvalue W_{pJ}, and E_k and W_s are defined just below Eq. (2.2).

The contribution to the integral of the matrix element of the electric multipole moment in Eq. (2.3),

$$\langle \Psi_{k,s,lm} | \sum_i r_i^\lambda Y_{\lambda\mu}^*(\Omega_r) | \Psi_{J_0 M_0} \rangle,$$

comes in general from the external region $r>a_s$. However, if we choose the channel radius a_s reasonably large so that the higher levels are not contaminated, then we may safely disregard the contribution of the external region and take $\Psi_{k,s,lm}$ to be given by Eq. (3.11). Thus,

$$\langle \Psi_{k,s,lm} | \sum_i r_i^\lambda Y_{\lambda\mu}^*(\Omega_r) | \Psi_{J_0 M_0} \rangle = \sum_{p,J,M} C_{kslm,pJM}^* \times \langle \Phi_{pJM} | \sum_i r_i^\lambda Y_{\lambda\mu}^*(\Omega_r) | \Psi_{J_0 M_0} \rangle. \tag{3.13}$$

Rigorously speaking, it must be demonstrated that the choice of the large a_s required by the neglect of the exterior region in the calculation of Coulomb excitation is consistent with the requirement that the physical levels should be reproduced within the accuracy needed in the numerical application, because the larger a_s is, the more closely spread are the levels. However, as we show later in the example of $^6\text{Li} \rightarrow \alpha + d$, the above treatment seems to be proper in an approximate sense, and we assume that the individual pJM terms in Eq. (3.13) with smaller excitation energies and small Γ_{pJ}'s represent Coulomb excitations with subsequent decays, which have been discussed by Gluckstern and Breit. Summation over many highly excited levels in Eq. (3.13) may represent more direct Coulomb disintegration processes.

IV. DIFFERENTIAL CROSS SECTION

A classical orbit in the Coulomb field is determined by two parameters, the impact parameter b and the angle φ_b which characterizes the direction of the orbital plane (see Fig. 1).

The differential cross section of a disintegration process, in which an incoming nucleus in an orbit defined by (b,φ_b) breaks up into the channel s, and product nuclei fly away so that the energy of the relative motion has the values between E_k and E_k+dE_k while the relative momentum vector points into the solid-angle element $d\Omega_k$ measured from the asymptotic direction of the classical orbit, is now given by

$$d\sigma = b db d\varphi_b dP(k,s,j_s m_s, d\Omega_k). \tag{4.1}$$

The probability of disintegration, $dP(k,s,j_s m_s,d\Omega_k)$, can

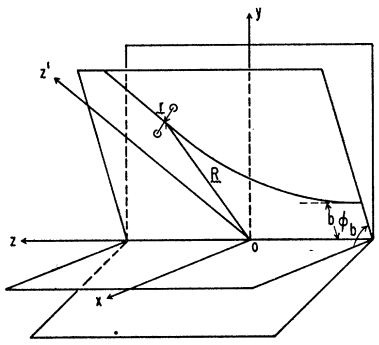

FIG. 1. A classical Rutherford trajectory in the Coulomb field of the target nucleus.

be written as[8]

$$dP(k,s,j_sm_s,d\Omega_k)=dE_kd\Omega_k\frac{1}{2J_0+1}\sum_{M_0}\sum_{m_s}\Big|\sum_{l,m}b_{k,s,j_sm_s,lm}e^{-\frac{1}{2}il\pi+i\delta_{l,s}}Y_{lm}(\Omega_k)\Big|^2, \tag{4.2}$$

where the previous $b_{k,s,lm}$ is written in full as $b_{k,s,j_sm_s,lm}$. Also the previous δ_l is written as $\delta_{l,s}$ to show its dependence on the channel index s.

Now, using Eqs. (2.3), (3.12), and (3.13), it is found that

$$b_{k,s,j_sm_s,lm}=\frac{4\pi Ze^2}{i\hbar}\sum_{\lambda,\mu}(2\lambda+1)^{-1}S_{\lambda\mu}\sum_{pJ,M}(JM,\lambda\mu\,|\,J_0M_0)(j_sm_s,lm\,|\,JM)\langle pJ\|T_\lambda\|J_0\rangle$$
$$\times\frac{-\hbar^2a_s}{2\mu_s}\frac{\nu(k_s)e^{i\delta_{l,s}}}{\varphi_l^{(-)}(k_sa_s)}\Big(\int\tilde{\Phi}_{pJM}{}^*\chi_{s,l,JM}d\Omega_rd\xi\Big)^*\Big/N_{pJ}(E_k+W_s-\mathcal{E}_{pJ}-\tfrac{1}{2}i\Gamma_{pJ}), \tag{4.3}$$

and thus, from Eq. (4.1), we obtain

$$d\sigma=bdbd\varphi_bdE_kd\Omega_k\frac{1}{2J_0+1}\sum_{M_0}\sum_{ms}\Big(\frac{4\pi Ze^2}{\hbar}\Big)^2\Big|\sum_{pJ,M}\sum_{l,m}\sum_{\lambda,\mu}(2\lambda+1)^{-1}\langle pJ\|T_\lambda\|J_0\rangle(-i)^l(JM,\lambda\mu\,|\,J_0M_0)(j_sm_s,lm\,|\,JM)$$
$$\times S_{\lambda\mu}Y_{lm}(\Omega_k)\frac{-\hbar^2a_s}{2\mu_s}\frac{\nu(k_s)e^{i\delta_{l,s}}}{\varphi_l^{(-)}(k_sa_s)}\Big(\int\tilde{\Phi}_{pJM}{}^*\chi_{s,l,JM}d\Omega_rd\xi\Big)^*\Big/N_{pJ}(E_k+W_s-\mathcal{E}_{pJ}-\tfrac{1}{2}i\Gamma_{pJ})\Big|^2. \tag{4.4}$$

In deriving these formulas, we have put

$$\langle\Psi_{pJM}\,|\sum_i r_i^\lambda Y_{\lambda\mu}{}^*(\Omega_r)\,|\,\Psi_{J_0M_0}\rangle=(JM,\lambda\mu\,|\,J_0M_0)\langle pJ\|T_\lambda\|J_0\rangle, \tag{4.5}$$

where $\langle pJ\|T_\lambda\|J_0\rangle$ is the reduced matrix element.

The phase factor $e^{i\delta_{l,s}}$ in Eq. (4.4), when necessary, can be obtained by requiring the continuity of the external solution Eq. (3.6) and the internal solution Eq. (3.11) on the channel surface $r=a_s$, as mentioned previously.

Equation (4.4) is quite general whenever our classical description of the motion of the center of mass of the incident nucleus is justified, and Eq. (4.4) contains modes of disintegration through the intermediate excitations of discrete excited states, as well as more direct disintegration modes.

In the following, however, we confine ourselves to discussion of disintegration only through those low-lying discrete excited levels which contribute mainly to the processes to be analyzed later.

In these cases, we can simplify Eq. (4.4) in the following ways: (i) We disregard the interference terms between different pJ terms, which is justified when the haziness of the identification of the pJ levels is not considered and it is not necessary to bring distant levels into consideration. In other words, when the sharp resonance terms do not overlap appreciably, this procedure appears reasonable. (ii) We also disregard the interferences between different l terms. This simplification seems to be justified by the following reasons: (i) The relative energy E_k is generally low, and higher l waves have smaller penetration factors, and so only the lowest l value is of importance; (ii) When some cluster property dominates, the lower excited levels may correspond to a single value of l, just as in the example of ^{6}Li; (iii) Phase shifts $\delta_{l,s}$ might have random values, so that interference terms between different l values would practically vanish.

After these simplifications, we obtain, in place of Eq. (4.4),

$$d\sigma=bdbd\varphi_bdE_kd\Omega_k\frac{1}{2J_0+1}\sum_{M_0}\sum_{ms}\Big(\frac{4\pi Ze^2}{\hbar}\Big)^2\sum_{pJ}\sum_{l}\frac{\Gamma_{pJ,sl}/2\pi}{(E_k+W_s-\mathcal{E}_{pJ})^2+(\frac{1}{2}\Gamma_{pJ})^2}\Big|\sum_M\sum_m\sum_{\lambda,\mu}(2\lambda+1)^{-1}$$
$$\times\langle pJ\|T_\lambda\|J_0\rangle(JM,\lambda\mu\,|\,J_0M_0)(j_sm_s,lm\,|\,JM)S_{\lambda\mu}(b)Y_{lm}(\Omega_k)\Big|^2, \tag{4.6}$$

in which

$$\Gamma_{pJ,sl}=\frac{\hbar^2a_s{}^2k_s}{\mu_s\,|\,\varphi_l^{(-)}(k_sa_s)\,|^2}\Big|\int\Phi_{pJM}{}^*\chi_{s,l,JM}d\Omega_rd\xi\Big|^2 \tag{4.7}$$

---

[8] N. F. Mott and H. S. W. Massey, *The Theory of Atomic Collisions* (Oxford University Press, London, 1965), 3rd ed., Chap. XXI.

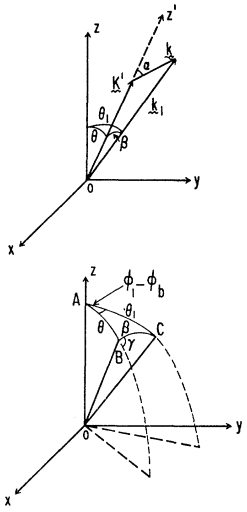

FIG. 2. Geometrical relations of the various momentum vectors.

is the partial width in the pJ level for the decay mode s, l. As mentioned previously, we can remedy our omission of the Coulomb repulsion between the disintegration products simply by assuming that the pJ level decays only into the Coulomb disintegration channel and using the experimentally determined value for $\Gamma_{pJ,s,l}$ in the right-hand side of Eq. (4.7). In Eq. (4.6), we have also put $N_{pJ}\simeq 1$ and disregarded the difference between $\tilde{\Phi}_{pJM}$ and Φ_{pJM}.

It may be worth while to remark that integrations of $d\sigma$ given above with respect to all variables give simply

$$\sigma=\sum_{pJ,s,l}(\Gamma_{pJ,s,l}/\Gamma_{pJ})\sigma_{pJ,\text{Coulomb}}. \tag{4.8}$$

$\sigma_{pJ,\text{Coulomb}}$ in Eq. (4.8), which is written as

$$\sigma_{pJ,\text{Coulomb}}=\tfrac{1}{4}a^2(4\pi Ze^2/\hbar)^2\sum_\lambda(2\lambda+1)^{-3}\times B_\lambda(E,J_0\rightarrow J)\sum_\mu|S_{\lambda\mu}|^2, \tag{4.9}$$

with

$$a=ZZ'e^2/(M_1+M_2)v_0^2,$$
$$B_\lambda(E,J_0\rightarrow J)=(2J_0+1)|\langle pJ\|T_\lambda\|J_0\rangle|^2, \tag{4.10}$$

is the well-known cross section of the Coulomb excitation for the level pJ, while $\Gamma_{pJ,sl}/\Gamma_{pJ}$ is the branching ratio of the decay of this level into the channel s with the angular momentum l.

Contrary to the simple result [Eq. (4.8)] for the total cross section, evaluation of the energy distribution and the angular distribution of one of the disintegration products needs much involved mathematical analysis, and this will be carried out in the following section.

V. ENERGY DISTRIBUTION AND ANGULAR DISTRIBUTION

Equation (4.6) is expressed in a coordinate system which is moving with the center of mass of the incident nucleus on a classical Coulomb trajectory. To obtain the energy distribution or the angular distribution of the product nucleus 1, we must, first, rewrite Eq. (4.6) with respect to the momentum variables and angle variables of the product nucleus 1, referred to the fixed coordinate system with its z axis pointing in the incident direction, and second, we must carry out the integration with respect to various Coulomb trajectories (see Fig. 1).

The momentum of the nucleus M_1, which we denote as $\hbar\mathbf{k}_1$, is the sum of the relative momentum $\hbar\mathbf{K}$ and $\hbar\mathbf{K}'$, the latter defined to be

$$\hbar\mathbf{K}'=(M_1/M_1+M_2)\hbar\mathbf{K}, \tag{5.1}$$

where $\hbar\mathbf{K}$ is the momentum vector pointing in the direction of the asymptote of the classical orbit and having the constant magnitude

$$\hbar K=[2(M_1+M_2)E_0]^{1/2}. \tag{5.2}$$

E_0 is the kinetic energy of the incident nucleus. We assume, throughout this paper, that the target nucleus is infinitely heavy.

Thus we have

$$\mathbf{k}_1=\mathbf{k}+\mathbf{K}'. \tag{5.3}$$

The geometrical relations of the above three vectors are illustrated in Fig. 2.

Direction angles for $\mathbf{k}_1$ and $\mathbf{K}'$ are (θ_1,φ_1) and (θ,φ_b), respectively, while those for $\mathbf{k}$, referred to the polar axis z', are (α,γ). The angle between $\mathbf{K}'$ and $\mathbf{k}_1$ is denoted by β.

Now it can be easily shown that

$$\begin{aligned}dE_k d\Omega_k&=\hbar^2k/\mu_s dk\,\sin\alpha d\alpha d\gamma\\&=\hbar^2k_1^2/\mu_s k dk_1\sin\beta d\beta d\gamma\\&=M_1k_1/\mu_s k dE_1\sin\beta d\beta d\gamma,\end{aligned} \tag{5.4}$$

which are useful relations for the purpose of carrying out the integrations in Eq. (4.6).

$bdbd\varphi_b$ in its turn can also be transformed to the variables $d\theta_1$, $d\varphi_1$ as follows:

$$bdbd\varphi_b=a^2f(\theta_1,\varphi_1,\beta,\gamma)\sin\theta_1 d\theta_1 d\varphi_1, \tag{5.5}$$

with $f(\theta_1,\varphi_1,\beta,\gamma)$ defined by

$$f(\theta_1,\varphi_1,\beta,\gamma)=\frac{1-\cos\beta\cos\theta_1-\sin^2\beta\sin^2\gamma+\sin\beta\cos\gamma(\sin^2\theta_1-\sin^2\beta\sin^2\gamma)^{1/2}}{(\cos\beta-\cos\theta_1)^3}\times\frac{\sin\beta\cos\gamma+(\sin^2\theta_1-\sin^2\beta\sin^2\gamma)^{1/2}}{(\sin^2\theta_1-\sin^2\beta\sin^2\gamma)^{1/2}}. \tag{5.6}$$

The derivation of this expression is given in the Appendix.

To rewrite Eq. (4.6) completely in the variables, $E_1(=\hbar^2k_1^2/2M_1)$, θ_1, φ_1, β, γ, the following relations are further

of use:

$$k=(K'^2+k_1^2-2K'k_1\cos\beta)^{1/2}, \tag{5.7}$$

$$\cos\alpha=(k_1^2-K'^2-k^2)/2K'k, \tag{5.8}$$

$$b=a\cot(\theta/2)=a\frac{\sin\beta\cos\gamma+(\sin^2\theta_1-\sin^2\beta\sin^2\gamma)^{1/2}}{\cos\beta-\cos\theta_1}, \tag{5.9}$$

where the last relation [Eq. (5.9)] is derived also in the Appendix.

Integration of Eq. (4.6) with respect to various Coulomb trajectories for the fixed values of θ_1, φ_1 now corresponds to integration with respect to the variables β and γ, which correspondence can also be understood from Fig. 2.

The differential cross section which is convenient for the discussion of energy distribution or angular distribution is thus found to be

$$d\sigma(k_1,\theta_1,\varphi_1)=\int\int\frac{d\sigma}{d\Omega(\beta,\gamma)}\sin\beta d\beta d\gamma, \tag{5.10}$$

$$\frac{d\sigma}{d\Omega(\beta,\gamma)}=a^2\left(\frac{4\pi Ze^2}{\hbar}\right)^2\frac{M_1k_1}{\mu_sk}f(\theta_1,\varphi_1,\beta,\gamma)dE_1d\Omega_1\sum_{pJ,l}\frac{\Gamma_{pJ,sl}/2\pi}{(E_k+W_s-\mathcal{E}_{pJ})^2+(\frac{1}{2}\Gamma_{pJ})^2}\frac{1}{2J_0+1}\sum_{M_0}\sum_{ms}\Big|\sum_{M}\sum_{m}\sum_{\lambda,\mu}(2\lambda+1)^{-1}$$
$$\times\langle pJ\|T_\lambda\|J_0\rangle(JM,\lambda\mu\,|\,J_0M_0)(j_sm_s,lm\,|\,JM)S_{\lambda\mu}(\theta,k)Y_{lm}(\cos\alpha,\gamma)\Big|^2. \tag{5.11}$$

$S_{\lambda\mu}$ in this formula is given by

$$S_{\lambda\mu}(\theta,k)=\frac{1}{v_0a^\lambda}\sum_{\mu'}D_{\mu'\mu}{}^\lambda(-\tfrac{1}{2}\pi-\tfrac{1}{2}\theta,\,-\tfrac{1}{2}\pi,\,-\tfrac{1}{2}\pi)Y_{\lambda\mu'}(\tfrac{1}{2}\pi,0)I_{\lambda\mu'}(\theta,\xi), \tag{5.12}$$

where $D_{\mu'\mu}{}^\lambda$ is the well-known matrix representation of the rotation operator, while the integral

$$I_{\lambda\mu'}(\theta,\xi)=\int_{-\infty}^{\infty}e^{i\xi(\epsilon\sinh w+w)}\frac{[\cosh w+\epsilon+i(\epsilon^2-1)\sinh w]^{\mu'}}{(\epsilon\cosh w+1)^{\lambda+\mu'}}dw,$$

with

$$\epsilon=(1/\sin\tfrac{1}{2}\theta),\quad \xi=(a/\hbar v_0)(E_k+W_s-W_0) \tag{5.13}$$

has already been evaluated and tabulated[1] for important values of parameters.

VI. A USEFUL LIMITING CASE

The main complexity of Eq. (5.11) arises from the circumstance that $S_{\lambda\mu}(\theta,k)$ and $Y_{lm}(\cos\alpha,\gamma)$ depend, through the relations in Eqs. (5.7), (5.8), and (5.9), on the variables β, γ. The very complex structure of Eq. (5.11) makes it desirable to search for some limiting cases which might lead to simpler results.

We assume, for this purpose, that $\mathcal{E}_{pJ}\geq W_s$, or that the available kinetic energy for the relative motion of the product pair of nuclei is very small, in the sense that $k\ll K'$. In this case, as can be seen from Fig. 2, the angle β remains always very small, irrespective of the direction of the vector $\mathbf{k}$. Thus, when we take the limit $\beta\to 0$, Eq. (5.6) and Eq. (5.9) show that $f(\theta_1,\varphi_1,\beta,\gamma)\to(1-\cos\theta_1)^{-2}=\frac{1}{4}\sin^{-4}\frac{1}{2}\theta_1$, as $\theta\to\theta_1$.

Now, in this limit, Eq. (5.11) is simplified to the following expression:

$$\frac{d\sigma}{d\Omega(\beta,\gamma)}=\tfrac{1}{4}a^2\left(\frac{4\pi Ze^2}{\hbar}\right)^2\frac{M_1k_1dE_1}{\mu_sk}\frac{d\Omega_1}{\sin^4\frac{1}{2}\theta_1}\sum_{pJ,l}\frac{\Gamma_{pJ,sl}/2\pi}{(E_k+W_s-\mathcal{E}_{pJ})^2+(\frac{1}{2}\Gamma_{pJ})^2}\frac{1}{2J_0+1}\sum_{M_0}\sum_{ms}\Big|\sum_{M}\sum_{m}\sum_{\lambda,\mu}(2\lambda+1)^{-1}$$
$$\times\langle pJ\|T_\lambda\|J_0\rangle(JM,\lambda\mu\,|\,J_0M_0)(j_sm_s,lm\,|\,JM)S_{\lambda\mu}(\theta_1,k)Y_{lm}(\cos\alpha,\gamma)\Big|^2. \tag{6.1}$$

In heavy-ion reactions the incident energy $E_0=\hbar^2k^2/2(M_1+M_2)$ frequently has a magnitude from several MeV to about 10 MeV per nucleon, while $\mathcal{E}_{pJ}-W_s$ remains several MeV. Thus our assumption $k\ll K'$ is not too restrictive, but is satisfied in many cases of interest. Our numerical calculations for the case $^6\mathrm{Li}\to\alpha+d$ in the following section will also be done starting from Eq. (6.1).

We now turn to the Gluckstern-Breit calculation referred to in the introduction and examine the relationships between their cross section and ours given by Eq. (6.1).

For very sharp levels with small Γ_{pJ}, one may use the approximation

$$((E_k+W_s-\mathcal{E}_{pJ})^2+(\Gamma_{pJ}/2)^2)^{-1}\to(2\pi/\Gamma_{pJ})\delta(E_k+W_s-\mathcal{E}_{pJ}), \tag{6.2}$$

through which the k's in Eq. (6.1) can be replaced by $k_s=(2\mu_s E_s)^{1/2}/\hbar$, with $E_s\equiv\mathcal{E}_{pJ}-W_s$. Then integration with respect to β and γ can be easily performed and we obtain, for $K'-k_s<k_1<K'+k_s$,

$$d\sigma(E_1,\Omega_1)=\tfrac{1}{4}a^2\left(\frac{4\pi Ze^2}{\hbar}\right)^2\frac{M_1dE_1d\Omega_1}{\hbar^2K'k_s\sin^4\frac{1}{2}\theta_1}\sum_{pJ,l}\frac{\Gamma_{pJ,sl}}{\Gamma_{pJ}}\frac{1}{2J_0+1}\sum_{M_0}\sum_{m_s}\sum_{M}(j_sm_s,l\,M-m_s|JM)^2\int|Y_{l\,M-m_s}(\cos\alpha^*,\gamma)|^2d\gamma$$
$$\times\Big|\sum_{\lambda}(2\lambda+1)^{-1}\langle pJ|T_\lambda|J_0\rangle(JM,\lambda\,M_0-M|J_0M_0)S_{\lambda,M_0-M}(\theta_1,k_s)\Big|^2;\quad(6.3)$$

otherwise, we obtain

$$d\sigma(E_1,\Omega_1)=0.\quad(6.4)$$

In the above we have

$$\cos\alpha^*=(k_1^2-K'^2-k_s^2)/2K'k_s.\quad(6.5)$$

If we further disregard the k_1 dependence of $|Y_{l\,M-m_s}(\cos\alpha^*,\gamma)|^2$ by replacing it with its mean value,

$$(2l+1)^{-1}\sum_{M-m_s}|Y_{l\,M-m_s}|^2=1/4\pi,$$

then we can also perform the summations on M_0, M, m_s. Thus Eq. (6.3) is reduced to a much simpler formula:

$$d\sigma(E_1,\Omega_1)=\tfrac{1}{4}a^2\left(\frac{4\pi Ze^2}{\hbar}\right)^2\frac{M_1dE_1d\Omega_1}{\hbar^2K'k_s\sin^4\frac{1}{2}\theta_1}\sum_{pJ,l}\frac{\Gamma_{pJ,sl}}{2\Gamma_{pJ}}\sum_{\lambda}(2\lambda+1)^{-3}B_\lambda(E,J_0\to J)\sum_{\mu}|S_{\lambda\mu}(\theta_1,k_s)|^2,\quad(6.6)$$

for $K'-k_s<k_1<K'+k_s$, while otherwise,

$$d\sigma(E_1,\Omega_1)=0.\quad(6.7)$$

This is essentially Gluckstern and Breit's formula, which these authors have derived in a more elementary way.

Gluckstern and Breit's formula is an approximation where the breadth of the level Γ_{pJ} is disregarded, and gives, as shown by Eqs. (6.6) and (6.7), a rectangular energy distribution which vanishes outside $K'-k_s<k_1<K'+k_s$, or, written in the energy variable, outside

$$\left[\left(\frac{M_1E_0}{M_1+M_2}\right)^{1/2}-\left(\frac{M_2E_s}{M_1+M_2}\right)^{1/2}\right]^2<E<\left[\left(\frac{M_1E_0}{M_1+M_2}\right)^{1/2}+\left(\frac{M_2E_s}{M_1+M_2}\right)^{1/2}\right]^2.\quad(6.8)$$

In actual cases, however, the finiteness of the breadth of excited levels might affect the energy distribution and the angular distribution considerably, and some general discussion of this point will be worthwhile.

To make a rough estimation, let us replace all k-dependent factors in Eq. (6.1) (except the resonance denominator) with their values at $k=k_s$. Integration with respect to β and γ then gives

$$d\sigma(E_1,\Omega_1)=\int_0^{2\pi}d\gamma\int_0^{\pi}\frac{d\sigma}{d\Omega(\beta,\gamma)}\sin\beta d\beta$$
$$=\int_0^{2\pi}d\gamma\int_{E'}^{E''}\frac{d\sigma}{d\Omega(\beta,\gamma)}\frac{\mu_s}{\hbar^2K'k_1}dE_k$$
$$=\tfrac{1}{4}a^2\left(\frac{4\pi Ze^2}{\hbar}\right)^2\frac{M_1}{\hbar^2K'}\frac{dE_1d\Omega_1}{\sin^4\frac{1}{2}\theta_1}\sum_{pJ,l}\frac{1}{k_s}\left\{\int_{E'}^{E'}\frac{\Gamma_{pJ,sl}/2\pi}{(E_k-E_s)^2+(\frac{1}{2}\Gamma_{pJ})^2}dE_k\right\}\frac{1}{2J_0+1}\sum_{M_0}\sum_{m_s}\int_0^{2\pi}d\gamma$$
$$\times\Big|\sum_{M}\sum_{m}\sum_{\lambda,\mu}(2\lambda+1)^{-1}\langle pJ\|T_\lambda\|J_0\rangle(JM,\lambda\mu|J_0M_0)(j_sm_s,lm|JM)S_{\lambda\mu}(\theta_1,k_s)Y_{lm}(\cos\alpha^*,\gamma)\Big|^2,\quad(6.9)$$

with

$$E'=\left[\left(\frac{M_1E_0}{M_2}\right)^{1/2}-\left\{\frac{(M_1+M_2)E_1}{M_2}\right\}^{1/2}\right]^2,\quad E''=\left[\left(\frac{M_1E_0}{M_2}\right)^{1/2}+\left\{\frac{(M_1+M_2)E_1}{M_2}\right\}^{1/2}\right]^2.\quad(6.10)$$

The energy integral in Eq. (6.9) is easily evaluated to be

$$F(E_1)\equiv\int_{E'}^{E''}\frac{\Gamma_{pJ,sl}/2\pi}{(E_k-E_s)^2+(\frac{1}{2}\Gamma_{pJ})^2}dE_k=\frac{\Gamma_{pJ,sl}}{\pi\Gamma_{pJ}}\arctan\frac{2(E''-E')/\Gamma_{pJ}}{1+4(E''-E_s)(E'-E_s)/\Gamma_{pJ}^2},\quad(6.11)$$

which represents the main E_1 dependence of the differential cross section $d\sigma(E_1,\Omega_1)$ and replaces the rectangular distribution in the previous δ-function approximation. The general behavior of $F(E_1)$ is shown in Fig. 3 for the case $E_0 \gg E_s > \Gamma_{pJ}$. The energy distribution has its center at about $M_1E_0/(M_1+M_2)$, and the breadth

$$\Delta E_1 = \left[\frac{12M_1M_2}{(M_1+M_2)^2}E_0E_s\right]^{1/2}.$$

These parameters are useful for the identification of resonance levels which contribute to the disintegration process. δE_1 in Fig. 3 contains a factor Γ_{pJ}/E_s; thus the rectangular shape of Gluckstern and Breit's calculation is expected to appear whenever $\Gamma_{pJ} \ll E_s$.

It is to be remarked that, while $F(E_1)$ given by Eq. (6.11) is the main E_1-dependent factor in Eq. (6.9), the latter formula contains other E_1-dependent factors $[S_{\lambda\mu}(\theta_1,k_s)$ and $Y_{lm}(\cos\alpha^*,\gamma)]$ which will give some modulation, difficult to predict, to the energy distribution curve.

In this situation we shall give, in the next section, results of our numerical calculations for the case of $^6\mathrm{Li} \rightarrow \alpha+d$, which is just the case discussed by Gluckstern and Breit.

VII. APPLICATION TO THE COULOMB DISINTEGRATION $^6\mathrm{Li} \rightarrow \alpha+d$

We carry out numerical calculations, starting directly from Eq. (6.1). Here, we take account of the k dependence of $S_{\lambda\mu}(\theta_1,k)$ and $Y_{lm}(\cos\alpha,\gamma)$. Our differential cross section is now expressed by

$$d\sigma(E_1,\Omega_1) = \tfrac{1}{4}a^2\left(\frac{4\pi Ze^2}{h}\right)^2 \frac{M_1}{h^2K'}\frac{dE_1d\Omega_1}{\sin^4\frac{1}{2}\theta_1}\sum_J \frac{1}{k_s}\frac{B_\lambda(E, J_0 \rightarrow J)}{(2J_0+1)^2(2\lambda+1)^2}\int_{E'}^{E''}\frac{\frac{1}{2}\Gamma_J}{(E_k-E_s)^2+(\frac{1}{2}\Gamma_J)^2}$$

$$\times\left\{\sum_{M_0}\sum_{M}\sum_{m_s}(j_sm_s, lM-m_s|JM)^2\int_0^{2\pi}|Y_{l,M-m_s}(\cos\alpha,\gamma)|^2d\gamma(JM, \lambda M_0-M|J_0M_0)^2|S_{\lambda\, M_0-M}(\theta_1,k)|^2\right\}dE_k. \quad (7.1)$$

Following Gluckstern and Breit, we take three excited states of ^{6}Li with $T=0$ and $J=3^+$, 2^+, 1^+, as are shown in Fig. 4.

We have omitted the suffix p and the excited levels are simply denoted by J. The partial width $\Gamma_{J,sl}$ is identified with the total width Γ_J, because the γ-ray width is extremely small. Only one value of l, namely $l=2$, is assumed. Accordingly, the value of λ is also set equal to 2.

The values of E_s and Γ_J are shown in Table I, and we see that the condition $\Gamma_J \ll E_s$, which is necessary for the δ-function approximation of the resonance factor, is very well satisfied for the first excited state, but not so well for higher levels.

In Fig. 5, energy distributions and angular distributions of the emitted α particles are shown for some emitted angles and energies for 61-MeV and 32-MeV incident ^{6}Li energies. For the 3^+ state we approximate the resonance factor in Eq. (7.1) with a δ function, which leads, naturally, to the same results that Gluckstern and Breit have already obtained. The energy-integrated total angular distribution remains essentially the same as that of Gluckstern and Breit. The main difference, however, appears in the shape of the energy distributions when ^{6}Li disintegrates through the excited states 2^+ and 1^+. In these cases the rectangular energy distributions are replaced by the smoothly tailed ones, as

TABLE I. Values of E_s and Γ for each excited level of ^{6}Li.

J^π	E_s (MeV)	Γ (MeV)
3^+	0.71	0.02
2^+	3.05	0.6
1^+	4.03	1.0

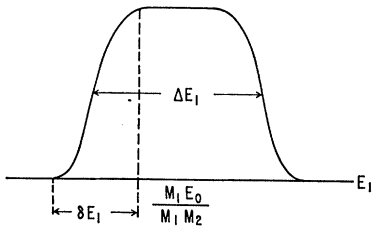

FIG. 3. Behavior of the function $F(E_1)$, where $\Delta E_1=[\{12M_1M_2/(M_1+M_2)^2\}E_0E_s]^{1/2}$, $\delta E_1=\frac{1}{6}\pi(\Gamma_{pJ}/E_s)\Delta E_1$.

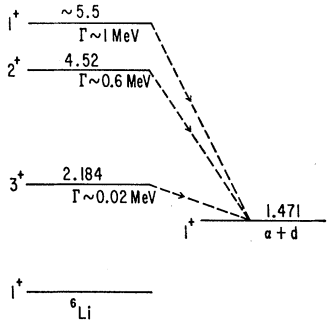

FIG. 4. Level scheme of ^{6}Li.

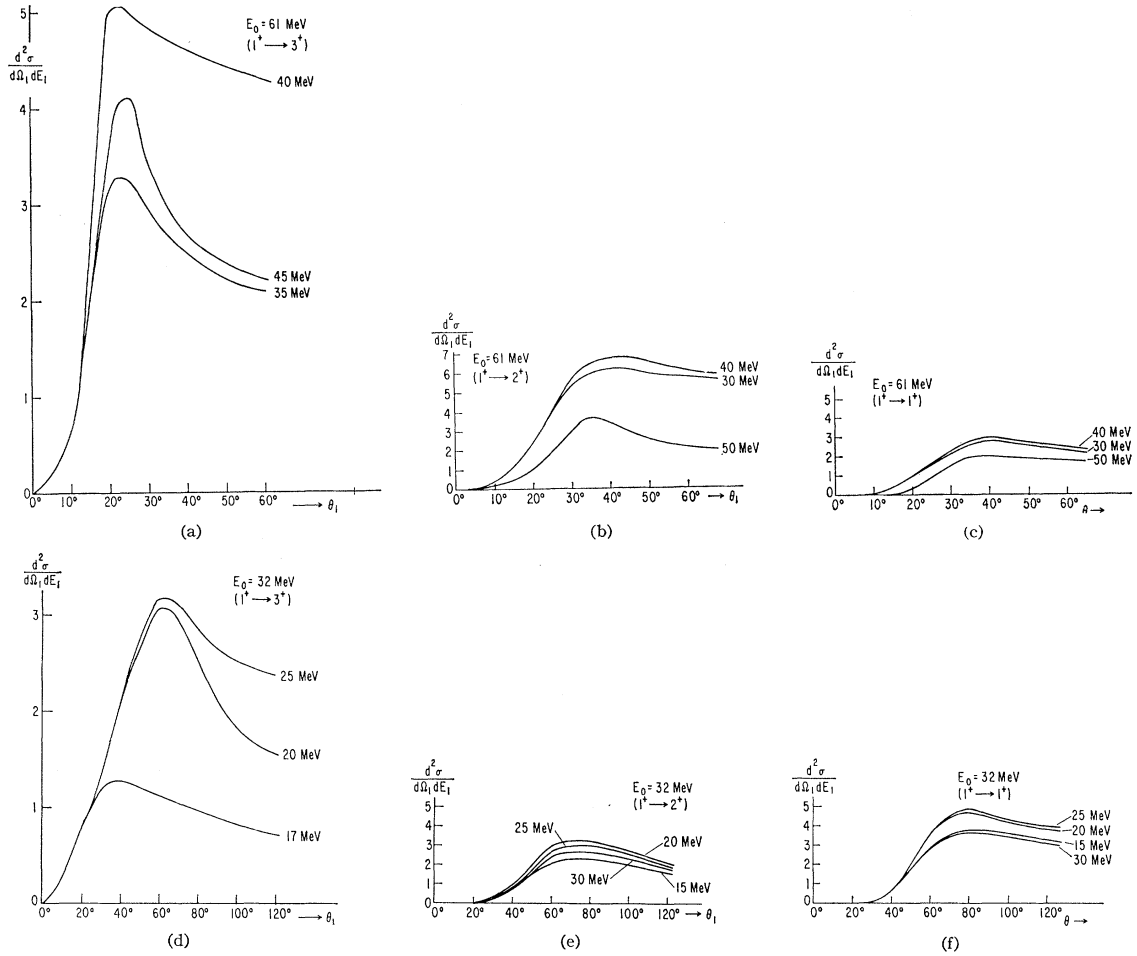

FIG. 5. (a) Calculated angular distributions of emitted α particles for $1^+ \rightarrow 3^+$ transition: $E_0=61$ MeV; $E_1=35$, 40, and 45 MeV. (b) Calculated angular distributions of emitted α particles for $1^+ \rightarrow 2^+$ transition: $E_0=61$ MeV; $E_1=30$, 40, and 50 MeV. (c) Calculated angular distributions of emitted α particles for $1^+ \rightarrow 1^+$ transition: $E_0=61$ MeV; $E_1=30$, 40, and 50 MeV. (d) Calculated angular distributions of emitted α particles for $1^+ \rightarrow 3^+$ transition: $E_0=32$ MeV; $E_1=17$, 20, and 25 MeV. (e) Calculated angular distributions of emitted α particles for $1^+ \rightarrow 2^+$ transition: $E_0=32$ MeV; $E_1=15$, 20, 25, and 30 MeV. (f) Calculated angular distributions of emitted α particles for $1^+ \rightarrow 1^+$ transition: $E_0=32$ MeV; $E_1=15$, 20, 25, and 30 MeV. (g) Calculated energy distributions of emitted α particles for $1^+ \rightarrow 3^+$ transition: $E_0=61$ MeV; $\theta_1=20°$, 30°, 40°, and 60°. (h) Calculated energy distributions of emitted α particles for $1^+ \rightarrow 2^+$ transition: $E_0=61$ MeV; $\theta_1=20°$, 30°, 40°, and 60°. (i) Calculated energy distributions of emitted α particles for $1^+ \rightarrow 1^+$ transition: $E_0=61$ MeV; $\theta_1=20°$, 30°, 40°, and 60°. (j) Calculated energy distributions of emitted α particles for $1^+ \rightarrow 3^+$ transition: $E_0=32$ MeV; $\theta_1=20°$, 60°, 80°, 100°, and 120°. (k) Calculated energy distributions of emitted α particles for $1^+ \rightarrow 2^+$ transition: $E_0=32$ MeV; $\theta_1=60°$, 80°, 100°, and 120°. (l) Calculated energy distributions of emitted α particles for $1^+ \rightarrow 1^+$ transition: $E_0=32$ MeV; $\theta_1=60°$, 80°, 100°, and 120°.

were roughly shown by Eq. (6.11) and in Fig. 3. The effects of the non-δ-function approximation are more conspicuous for the 1^+ state than the 2^+ state and for 61 MeV than 32 MeV, as is also readily understood from examining Eq. (6.11).

As long as we confine ourselves to first-order perturbation theory, these modifications remain unimportant because of the small intensities of $1^+ \rightarrow 2^+$, $1^+ \rightarrow 1^+$ transitions relative to that of $1^+ \rightarrow 3^+$. However, as will be discussed later, these intensity ratios are modified considerably by the higher order effect, and tailings of the $1^+ \rightarrow 2^+$ and $1^+ \rightarrow 1^+$ distributions will make remarkable contributions to the total distribution.

VIII. DISCUSSION ON HIGHER ORDER APPROXIMATIONS AND NUCLEAR EFFECT

All calculations in the previous sections are the first-order perturbation calculations of Coulomb excitation and the subsequent decay of the excited levels. Here we would like to give some qualitative discussion about the validity of the first-order approximation and the possible consequences of the higher order effects.

One of the important higher order effects for our problem is the damping effect. It is known[9] from a formal viewpoint that the second-order reorientation effect associated with transitions among the sublevels of the

[9] G. Breit and J. P. Lazarus, Phys. Rev. **100**, 942 (1955).

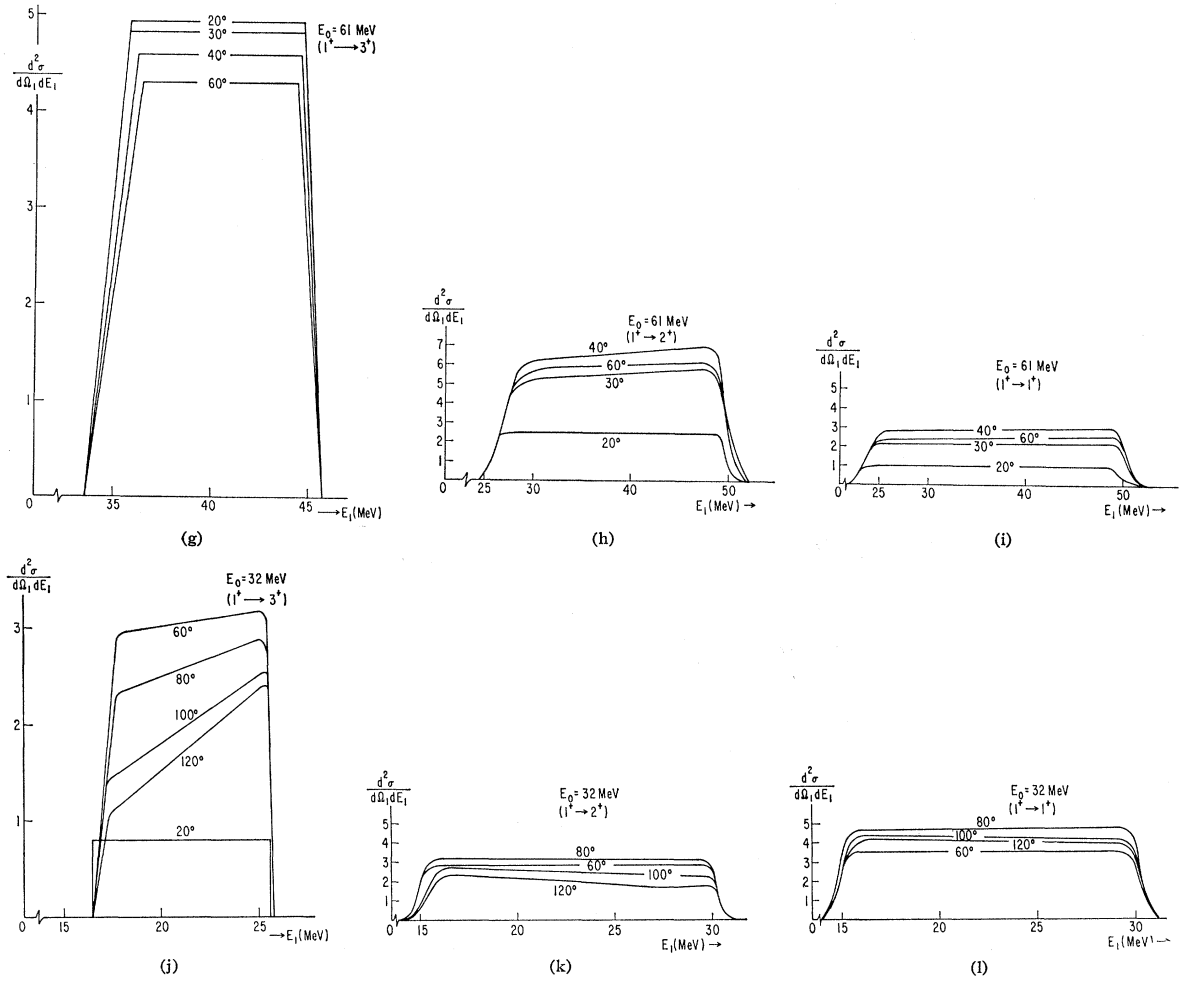

Figure 5 (*continued*).

excited states is of the same order as the de-excitation effect. Since no energy change is involved in the former, transitions among the various magnetic sublevels are favored. The fact that these two effects enter in the same order of the Coulomb excitation has been examined in detail by Breit and Gluckstern.[7] Even if the transitions between magnetic substates are neglected, it still may be worth while to mention the importance of the effect of the finite lifetime of the upper levels, at least in the ^{6}Li case. We can illustrate this in a qualitative and intuitive way.

Let us introduce $\gamma_J(b)/\hbar$, the probability per unit time for the Coulomb de-excitation of an excited level J to the ground state when the nucleus moves along the Coulomb orbit with impact parameter b. A necessary condition for the validity of the previous first-order calculation is

$$\Gamma_J \gg \gamma_J(b), \tag{8.1}$$

or, in other words, that the disintegration takes place so rapidly that the excited nucleus does not have enough time to make a second Coulomb interaction with the target nucleus going back again to the ground state. Otherwise, we must take into account the probability of this backward process, which will introduce a factor

$$\Gamma_J/[\Gamma_J+\gamma_J(b)] \tag{8.2}$$

multiplied by the first-order disintegration probability.

Of course, the definition of the probability per unit time $\gamma_J(b)$ in the framework of our classical method is not quite evident, because there the probability of a transition is given only through the time integral from $t=-\infty$ to $t=+\infty$ in Eq. (2.4). Nevertheless, for our qualitative argument, we can conclude that the main contributions to the time integral come only from the rather narrow integration domain near $t=0$; that is, from the time interval while the incident nucleus traverses the portion of its path located near the point of the closest approach, separated by the distance $R_{\min}$ from the center of mass of the target nucleus. Then it is plausible to take the effective path length as also comparable to $R_{\min}$.

TABLE II. Values of de-excitation probability per unit time for each excited level for typical scattering angles.

θ_1 \ J^π	3^+	2^+	1^+
	(a) $E_0=61$ MeV		
20°	0.0028	0.0018	0.00075
30°	0.082	0.019	0.0096
40°	0.23	0.080	0.041
60°	0.90	0.36	0.19
	(b) $E_0=32$ MeV		
20°	0.000075	~0	~0
60°	0.031	0.0013	0.00018
80°	0.070	0.0037	0.00060
100°	0.098	0.0057	0.00095
120°	0.10	0.0057	0.00096

As is well known, $R_{\min}$ varies with the scattering angle θ as

$$R_{\min}=a(1+[1/\sin\tfrac{1}{2}\theta]). \tag{8.3}$$

Thus, $\gamma_J(b)$ is obtained by equating

$$[\gamma_J(b)/\hbar]\times(\text{time of flight through the effective length of orbit})=(\text{total de-excitation probability } P_{J\to J_0}). \tag{8.4}$$

Now, the time of flight through the path length $R_{\min}$ is given by $R_{\min}/v$, where v is the orbital velocity at the point of the closest approach, which is obtained from the conservation of angular momentum, $R_{\min}v=bv_0$. Thus, Eq. (8.4) becomes

$$[\gamma_J(b)/\hbar][R_{\min}^2/bv_0]=P_{J\to J_0},$$

or, remembering $b=a\cot\frac{1}{2}\theta$,

$$\gamma_J(\theta)=(E_0/\eta)P_{J\to J_0}(\theta)\sin\theta/[1+\sin(\theta/2)]^2, \tag{8.5}$$

where $\eta=ZZ'e^2/\hbar v_0$. Table II shows $\gamma_J(\theta)$ for typical values of the parameters and Table III shows corresponding values of $\Gamma_J/[\Gamma_J+\gamma_J(\theta)]$. In this calculation we used the value of $P_{J\to J_0}(\theta)$ which Gluckstern and Breit have estimated: that is, $P=0.05$ for $\theta=30°$, $J=3$, $E_{\mathrm{Li}}=61$ MeV, and $P=0.21$ for $\theta=120°$, $J=3$, $E_{\mathrm{Li}}=32$ MeV.[10]

TABLE III. Correction factors due to the damping effect for each disintegration process.

θ_1 \ J^π	3^+	2^+	1^+
	(a) $E_0=61$ MeV		
20°	0.88	1.0	1.0
30°	0.20	0.97	0.99
40°	0.080	0.88	0.96
60°	0.022	0.63	0.84
	(b) $E_0=32$ MeV		
20°	1.0	~1	~1
60°	0.39	1.0	1.0
80°	0.22	0.99	1.0
100°	0.17	0.99	1.0
120°	0.16	0.99	1.0

The intensity of $1^+\to 3^+$ is diminished considerably by the damping effect, while $1^+\to 2^+$ and $1^+\to 1^+$ are little affected, and this trend becomes more apparent for larger angles. Figures 6(a), 6(b), 7(a), and 7(b) show the corrections when the above analysis is applied to the Gluckstern-Breit first-order calculations in Ref. 5.

The above estimation of the damping effect is certainly approximate and too much reliance must not be given to the detailed quantitative results. The value of $B_2(E, 1^+\to 3^+)$ used by Gluckstern and Breit is about 10^{-50} cm^4, which is not unreasonable. This fact shows that the important part of the ejected α particles certainly comes from the Coulomb disintegration of ^{6}Li, which basically justifies use of the above values of P.

There are some other higher order effects which have so far been neglected in this treatment. First, our treatment involves a strong limitation on the number of low-lying excited states and it is not valid, in general, if the incident projectile is heavier than ^{6}Li, since the electric field surrounding the target nucleus becomes so intense that higher excitation processes are not negligible. And if the electric interaction becomes so strong that many levels are actively involved in the excitation process, one has to solve directly the set of coupled equations which describe the population of the nuclear states during the collision, as the Copenhagen group[1] has already pointed out.

To the second order of perturbation theory, the probability amplitude $b_{k,s,lm}^{(2)}$ for a transition from the initial state $\Psi_{k,s,lm}$ of the incident nucleus is given by

$$b_{k,s,lm}^{(2)}=b_{if}^{(1)}(\omega)+\textstyle\sum_n b_{inf}, \tag{8.6}$$

where $b_{if}^{(1)}(\omega)$ is used as the first-order amplitude instead of Eq. (2.2), and

$$b_{inf}=\frac{1}{(i\hbar)^2}\int_{-\infty}^{\infty}\langle\Psi_{k,s,lm}|H'(t)|\Psi_n\rangle e^{-i\omega_2 t}dt \times\int_{-\infty}^{t}\langle\Psi_n|H'(t')|\Psi_{J_0M_0}\rangle e^{-i\omega_1 t'}dt'. \tag{8.7}$$

The frequencies ω_1, ω_2, and ω are given by

$$\begin{aligned}\omega_1&=(W_0-W_n)/\hbar,\\ \omega_2&=(W_n-E_k-W_s)/\hbar,\\ \omega&=(W_0-E_k-W_s)/\hbar,\end{aligned} \tag{8.8}$$

where the energy of the intermediate state is denoted by W_n. The double integral in Eq. (8.7) is evaluated

[10] Numerals in the above tables are somewhat arbitrary because the employment of $R_{\min}/v$ for the collision time is arbitrary, as mentioned in the text. On this point see Ref. 7, especially Eqs. (9) and (10).

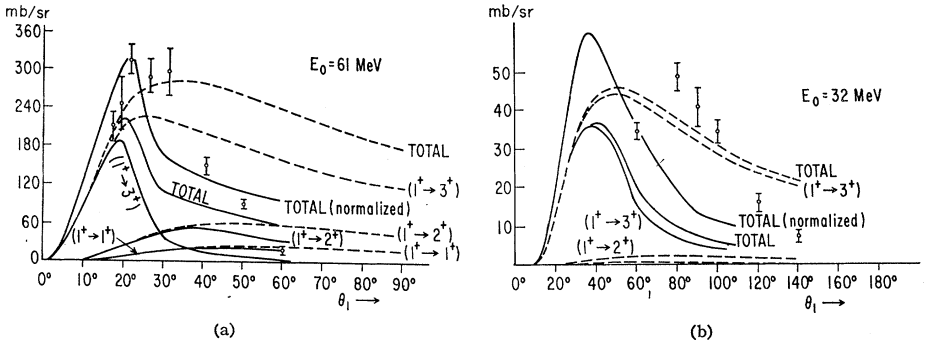

FIG. 6. Angular distributions comparing Gluckstern and Breit's results (dashed lines) with our calculations (solid lines). The curve "Total (normalized)" is arbitrarily normalized to approach the observed curve. (a) $E_0=61$ MeV. (b) $E_0=32$ MeV.

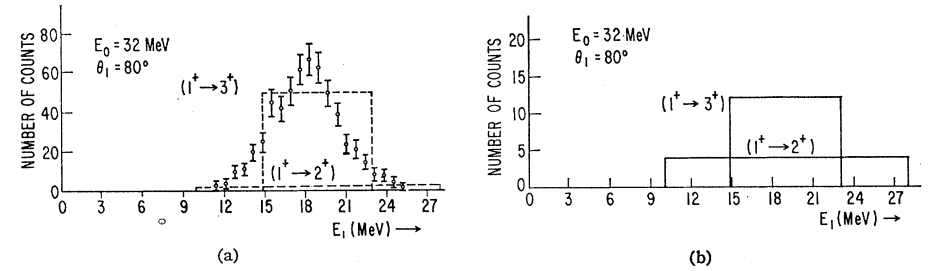

FIG. 7. (a) Energy distributions showing Gluckstern and Breit's results (dashed lines). (b) Energy distribution with our calculations (solid lines).

by Alder *et al.*[1] and it gives

$$b_{inf}=\tfrac{1}{2}b_{in}(\omega_1)b_{nf}(\omega_2)+\frac{i}{2\pi}\mathcal{P}\int_{-\infty}^{\infty}\frac{b_{in}(\omega_1+q)b_{nf}(\omega_2-q)}{q}dq, \quad (8.9)$$

where $\mathcal{P}$ stands for the principal part of the integral. The $b_{if}^{(1)}(\omega)$ is obtained from Eq. (2.3), (4.5), and (5.12), and is found to be

$$b_{if}^{(1)}(\omega)=(4\pi Ze^2/i\hbar v_0)\sum_{\lambda=1}^{\infty}\sum_{\mu=-\lambda}^{\lambda}\sum_{\mu'}(2\lambda+1)^{-1}\times(JM,\lambda\mu|J_0M_0)\langle pJ\|T_\lambda\|J_0\rangle a^{-\lambda}\times D_{\mu\mu'}{}^{\lambda}(-\tfrac{1}{2}\pi-\tfrac{1}{2}\theta,-\tfrac{1}{2}\pi,-\tfrac{1}{2}\pi)\times Y_{\lambda\mu'}(\tfrac{1}{2}\pi,0)I_{\lambda\mu'}(\theta,\xi). \quad (8.10)$$

Substituting Eq. (8.10) into Eq. (8.9) and inserting the result into Eqs. (4.2) and (4.1), the differential cross section to second order may be written as

$$d\sigma=d\sigma^{(1)}+d\sigma^{(1,2)}+d\sigma^{(2)}. \quad (8.11)$$

Here, the first term represents the first-order excitation cross section which we have already obtained in Eq. (4.4) or Eq. (4.6), the second term is the interference term between first-order and second-order differential cross sections, and the third term is the second-order excitation. These last two terms are explicitly calculated in the Copenhagen review,[1] and we know that if the intermediate energy levels are well above that of the final state, they may give a significant contribution to the total cross section.[11] This is because for large ξ, the ξ^{-1} in the second term of Eq. (8.9) is large compared to the exponentially decreasing function of ξ in $I_{\lambda\mu'}(\theta,\xi)$ in Eq. (8.10).

In the summation over the multipole orders, the main contribution to the second-order cross section will arise from the lowest λ permitted by the selection rules for the nuclear matrix elements, as is the case for the first-order cross section.

Next we shall touch on the multipole excitation by successive transitions leading to a final state, a process which may become important with increasing charge of the projectile. For instance, if a heavy-ion projectile with 0^+ spin and parity in its ground state has the 4^+ state in a collective band, it should be excited by two $E2$ transitions via the intermediate 2^+ state with quite high probability, even though the direct excitation of 4^+ state by a single $E4$ transition is very improbable. In this case, the double quadrupole excitation cross section may be obtained approximately from Eq. (8.9), on the basis of the semiclassical treatment, as

$$\sigma_{E2E2}(I_i\to I_n\to I_f)\approx(f_c/4a^2)\sigma_{E2}(I_i\to I_n)\times\sigma_{E2}(I_n\to I_f), \quad (8.12)$$

where f_c is a correction factor less than 1.[12] The importance of the double $E2$ transition compared to the direct $E4$ transition is easily seen if we evaluate their

[11] See Ref. 1 and also J. O. Newton, in *Nuclear Structure and Electromagnetic Interactions*, edited by N. MacDonald (Plenum Press, Inc., New York, 1965), pp. 287 ff.

[12] G. Breit and R. L. Gluckstern, in *Handbuch der Physik*, edited by S. Flugge (Springer-Verlag, Berlin, 1959), Vol. 41, Sec. 1, pp. 548 ff.

ratio. Using Eq. (8.12),

$$\frac{\sigma_{E4}(0\rightarrow 4)}{\sigma_{E2E2}(0\rightarrow 2\rightarrow 4)}\approx\left(\frac{\hbar v_0}{Z'e^2}\right)^2 \times\frac{e^2B_{0\rightarrow 4}(E4)}{f_cB_{0\rightarrow 2}(E2)B_{2\rightarrow 4}(E2)}, \quad (8.13)$$

in which the probability of cascade excitation versus crossover excitation rapidly increases as the charge of the projectile increases.

In our present case, however, we cannot examine the validity of the above theory of Coulomb disintegration by multiple-excitation processes because of the lack of the experimental data.

Furthermore, there remain to be studied other higher order effects. For example, the polarization of the incident nucleus in the intense Coulomb field is not as easy to estimate as the damping effect, and must be reserved for future study.

Another source of discrepancy would be the nuclear effect. This effect might be expected to become important when the distance of closest approach of the two particles is less than the sum of their radii. This is expected for large angles of α-particle emission (larger than 40° for $E_{\mathrm{Li}}\simeq 60$ MeV, larger than 110° for $E_{\mathrm{Li}}\simeq 30$ MeV), and hence a smaller angular region might correspond to pure Coulomb disintegration. However, the nuclear surface is certainly not sharp, and exponential tails of the nuclear potential would give rise to some modifications of the assumed Coulomb orbits. As was pointed out first by Kammuri,[13] such a nuclear potential is indeed essential for the interpretation of neutron-transfer reactions in high-energy heavy-ion collisions. The effects of such a nuclear potential for Coulomb excitations and Coulomb disintegrations remain to be studied.

Finally, we add here a short remark about a possible stripping mechanism which would give α-particle emission. For higher energy collisions of heavy ions, the attractive nuclear potential will certainly play an important role. Indeed, Kammuri has shown that in grazing collisions this attractive nuclear potential tends to cancel the repulsive Coulomb force, and the deflection angle of the incident particles in the pure Coulomb field approaches zero, instead of the finite angle θ determined by $\sin\frac{1}{2}\theta=(R/a-1)^{-1}$ (R is the sum of radii of two colliding nuclei, and a is defined in Sec. IV). Thus, we might expect that the stripped α particles would have a forward-peaked angular distribution, just as neutrons stripped off from high-energy deuterons exhibit a strong forward peaking. α particles observed by Knox[14] from Au to Rh bombarded by 160-MeV ^{16}O have shown just such strong forward peakings. On the other hand, preliminary estimates of Breit, McIntosh, and Rawitscher indicate[15] that stripping contributions in the case of $^6\mathrm{Li}\rightarrow\alpha+d$ may be comparable with the observed cross sections and angular distributions.

IX. CONCLUDING REMARKS

A general theory is given for the differential cross section for the Coulomb disintegration of a complex nucleus. The usual classical orbit method is employed to describe the motion of the center of mass of the incident nucleus in the Coulomb field of the target nucleus. The wave function for the final state, in which the incident nucleus splits into two fragments, is constructed from the compound-nucleus theory of Kapur and Peierls. First-order perturbation theory is used to obtain the differential cross section.

An explicit expression of the differential cross section is given for a special but practically important case, in which lower unstable excited states contribute to the disintegration process without appreciable interference. This expression is evaluated numerically to obtain the energy and angular distribution of ejected α particles when a gold target is bombarded by ^{6}Li ions of energy from 20 to 65 MeV. This seems to be the only existing data in which Coulomb disintegration would play an important role; indeed, Gluckstern and Breit's theory gives a general quantitative fit to the observed results along this approach.

Our numerical computations give results essentially analogous to the simplified theory of the above authors. Our energy spectrum of α particles (Fig. 5) has some fine distortion superimposed upon the Gluckstern and Breit spectrum, but considerable discrepancies from the observed results still remain unresolved as to the detailed behavior of the energy spectrum. Our angular distribution of α particles is found to be practically the same as that of the above authors.

Our expression for the differential cross section, discussed above, is obtained from first-order perturbation theory just as was that of Gluckstern and Breit. However, we require a more detailed analysis of the higher order effects than is presented here in order to obtain both qualitative and quantitative agreement with experiment.

Concerning one of the higher order effects, rough estimates are given for the case $^6\mathrm{Li}\rightarrow\alpha+d$ of the probability of the backward jump of a once-excited nucleus into the elastic-scattering channel. This probability is found to be very large and considerably affects the angular and the energy distributions of α particles computed in the first-order approximation. The effects of this damping correction applied to the first-order angular distributions and the energy distributions are shown in Figs. 6, 7(a), and 7(b), but we dare not insist

[13] T. Kammuri, Progr. Theoret. Phys. (Kyoto) **28**, 934 (1962).

[14] W. J. Knox, in *Proceedings of the Second Conference on Reactions between Complex Nuclei, 1960*, edited by A. Zucker, E. C. Halbert, and F. T. Howard (John Wiley & Sons, Inc., New York, 1960), p. 263.

[15] See Ref. 5, p. 81, item 4.

that this correction has improved the agreement with the observed results.

The intensity ratios between $1^+ \rightarrow 3^+$, $1^+ \rightarrow 2^+$, and $1^+ \rightarrow 1^+$ excitations are also affected considerably by the damping corrections, and hence the shape of the energy spectrum will change; but the observed sharply peaked spectrum cannot be reached through these corrections.

Concerning the stripping mechanism, it may give results which are not clearly negligible in comparison with electrodisintegration. Even though we grant that the stripping process and the electrodisintegration process give similar contributions to the Coulomb excitation cross section, we can only conclude that an analysis of the data cannot easily distinguish between the simultaneous presence of both effects and the presence of just one of them.

ACKNOWLEDGMENTS

The author is much indebted to Professor M. Nogami for his suggestion of the problem, kind guidance, and continuous interest and encouragement, and for his invaluable help throughout the course of the present work. He is also grateful to Professor T. Muto for his warm interest, encouragement, comments, and criticism. Thanks are due to Dr. Y. Nagaoka and Dr. J. L. Peacher for stimulating discussions. He expresses his deep thanks to Dr. T. Foster for careful reading of the manuscript and for many helpful suggestions. Finally, he would like to express his appreciation to the Institute for Radiation Physics and Aerodynamics, University of California, San Diego, La Jolla, where part of this work was carried out.

APPENDIX: DERIVATION OF EQUATION (5.6)

Figure 8 illustrates the relative orientations of $\mathbf{k}_1$ and $\mathbf{K}'$. The z axis is chosen in the direction of incidence.

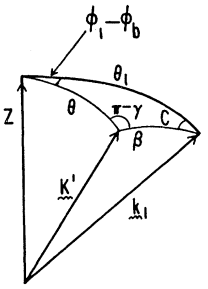

FIG. 8. Geometrical relations of the various momentum vectors and their angles.

From the spherical triangle, we get the following three relations:

$$\sin(\varphi_1-\varphi_b)=\sin\beta\,\sin\gamma/\sin\theta_1, \quad \text{(A1)}$$

$$\frac{\cos((\varphi_1-\varphi_b-\gamma+\pi)/2)}{\sin(C/2)}=\frac{\cos((\theta_1+\beta)/2)}{\cos\tfrac{1}{2}\theta}, \quad \text{(A2)}$$

$$\frac{\cos((\varphi_1-\varphi_b+\gamma-\pi)/2)}{\sin(C/2)}=\frac{\sin((\theta_1+\beta)/2)}{\sin\tfrac{1}{2}\theta}. \quad \text{(A3)}$$

Eliminating $\sin(C/2)$ from Eqs. (A2) and (A3), we obtain

$$\cot\tfrac{1}{2}\theta\,\tan(\tfrac{1}{2}(\theta_1+\beta))=\frac{\cos((\varphi_1-\varphi_b+\gamma-\pi)/2)}{\cos((\varphi_1-\varphi_b-\gamma+\pi)/2)}$$

or,

$$-\cot\tfrac{1}{2}\theta\,\tan(\tfrac{1}{2}(\theta_1+\beta))=\frac{\sin((\varphi_1-\varphi_b+\gamma)/2)}{\sin((\varphi_1-\varphi_b-\gamma)/2)}. \quad \text{(A4)}$$

From Eqs. (A1) and (A4) we can further eliminate $\varphi_1-\varphi_b$ and get

$$\cot\tfrac{1}{2}\theta=\frac{\sin\beta\,\cos\gamma\pm(\sin^2\theta_1-\sin^2\beta\,\sin^2\gamma)^{1/2}}{\cos\beta-\cos\theta_1}, \quad \text{(A5)}$$

in which the plus sign must be chosen for our cases of interest where β remains very small. Thus we obtain Eq. (5.9) and consequently Eq. (5.6) in the text.